Supplemental legend

Supplemental Figure S1

Meiotic progression in *snf22Δ*, *gcn5Δ*, *hrp3Δ*, and *ada2Δ* strains were monitored by DNA replication (FACS analysis), meiotic DNA double strand breaks (DSBs) formation, meiotic *rec* gene induction (Northern analysis), meiotic nuclear divisions and ascus formation. Because DSBs in wild type cells are repaired promptly, they can be difficult to detect (Cervantes *et al.*, 2000). Therefore we used a *pat1-114 rad50s* mutant strain, which allowed us to detect DSBs efficiently (Cervantes *et al.*, 2000). The mutation of *pat1-114* is suitable for the synchronous induction of meiosis (Iino and Yamamoto, 1985; McLeod and Beach, 1986). In the *rad50s* mutant strain, DSBs are not repaired and accumulate (Young *et al.*, 2002). The *pat1-114 rad50s* strain carrying following mutation, WT (PKH138), *snf22*• (S13-I1), *gcn5*• (TY24), *hrp3*• (PKH309), and *ada2*• (PKH310) were cultured to induce meiosis as described in supplemental Materials and methods. (A) Premeiotic DNA replication was monitored by FACS analysis. DNA content was increased to 2C between 2hr-3hr after induction of meiosis except for *snf22Δ* and *gcn5Δ*. In *snf22Δ* and *gcn5Δ*, DNA content was increased in slightly later timing. These results indicate that these mutants could enter meiotic cell cycle and progress normal pre-meiotic DNA synthesis (pre-meiotic S). (B) Whole DSBs were separated by pulse field gel electrophoresis (PFGE). Meiotic DSBs were appeared from 4-6 hr after induction of meiosis, indicating these mutants could introduce meiotic DSBs normally. (C) The transcripts of meiosis specific *rec* genes were detected by northern analysis. The transcripts of *rec6*, *rec7*, *rec8* and *rec12* were detected from 2hr (for *rec6*, *rec7*, *rec8*) or 4 hr (for *rec12*) after the induction of meiosis in wild type, while the induction of these meiotic genes (especially for *rec6*) were delayed and reduced in all mutants, indicating delayed and poor meiotic progression in these mutants. (D) Nuclear divisions were observed microscopically. The meiotic nuclear divisions were much delayed in these mutants in synchronous meiosis using *pat1-114* (data not shown). Since these mutants show slight temperature sensitive phenotype, it is possible that the delay in meiotic nuclear division is due to the high temperature condition in the synchronous meiosis (Mizuno *et al*., unpublished result). Therefore, we monitored the meiotic nuclear division in physiological condition using *pat1*$^{+}$ diploid strains. The *pat1*$^{+}$ diploid strains carrying following mutation, WT (D20), *ada2*• (D52), *hrp3*• (D53), and *snf22*• (D13A1B5) were cultured as in figure 1. A portion of the culture was harvested at indicated time points and

fixed by ethanol. The fixed cells were stained by Hoechst 33342 and observed under fluorescent microscopy. The graphs indicate the fractions of cells with one, two, or four nuclei at various time points after induction of meiosis. (E) We also observed ascus formation in *pat1*$^{+}$ *rad50*$^{+}$ back ground in these mutants. The haploids (h^{+} and h^{-}) carrying indicated mutations were mixed and spotted on SPA and cultured at 30^{o}C for 40 hr to induce mating and meiosis. The panels indicate the morphology of mating and sporulations. All mutants could generate regular ascus containing four spores. It should be noted that sporulation of *snf22•* was delayed and poor because of its deficiency in mating. Almost all zygotes in *snf22•* contain four spores, indicating successful completion of meiosis in this mutant. (bar=10μm) (F-G) To monitor the meiotic progression in the diploid, whole DSBs were analyzed using the *rad50s* diploid strains carrying indicated mutations. Each of the diploid strains was cultured in MM+N and shifted to MM-N to induce meiosis. Cells were harvested from each of the culture and divided into two portions. Following experiments (meiotic DSB detection and chromatin analysis) were performed using same culture. (F) Whole DSBs were separated by PFGE. Meiotic DSBs were appeared from 4 hr after nitrogen starvation in each of strains. (G) The chromatin analysis was performed using the culture at 0 and 8 hours after nitrogen starvation. In the *rad50s* diploid strain, the intense band at *M26* was appeared (indicated by arrowhead), similar to the wild type diploid strain (shown in figure1). In contrast, such chromatin remodeling at *M26* was impaired in *snf22•*. The amounts of whole DSBs in these mutants at 8 hours after nitrogen starvation seems larger or equivalent to that in wild type at 4 hours after nitrogen starvation when the drastic chromatin remodeling was observed in wild type diploid strain (shown in figure 1). These results indicate that chromatin remodeling at *M26* is impaired in *snf22•*. For the quantitative analysis, the intensity of each band at *M26* and downstream control band were quantified. The ratios of the intensity were indicated below the each lane.

Supplemental Figure S2

The initiation site of short transcript of *ade6-M26* was determined by 5'-race analysis as described in Supplemental Materials and Methods. The PCR product was cloned and sequenced using reverse primer located in *ade6* gene. The box and arrow indicate the CRE related heptanucleotid sequence created by *M26* mutation and its direction respectively. The red arrow indicates the initiation site of shorter RNA and that of

direction. The primer sequence used in RACE-PCR analysis was indicated by bracket.

Supplemental Figure S3

Stress-sensitive phenotypes of the *snf22*$^{+}$, *hrp1*$^{+}$, *hrp3*$^{+}$, *gcn5*$^{+}$, and *ada2*$^{+}$ deletion strains. We examined the effects of osmotic (1.2 M sorbitol), cation (1 M KCl), glucose starvation (0.1% glucose + 3% glycerol), oxidative (H_2O_2), replication (HU) and DNA damage (ultraviolet irradiation, UV, and methylmethane sulfonate, MMS) stresses. The isogenic haploid strains (*h*$^{+}$ *ade6-M26 his5-303*) carrying *gcn5*•, *snf22*•, *gcn5*•/*snf22*•, *hrp1*•, *hrp3*•• or *ada2*• were cultured in YE to mid-log phase and a diluted series (10-fold dilution) of the culture was spotted on plates containing various stress agents (indicated in panel). Then, 100 and 200 J/cm^2 of UV was irradiated to the cells on plates without stress agents. Spotted plates were cultured at 30° C for 3 or 4 days.

Supplemental Figure S4

Snf22 is required for proper cell-cycle arrest in response to nitrogen starvation and mating. (Upper panel) The haploid strains (wild type, *snf22*Δ, *ada2*Δ / *snf22*Δ, and *ada2*Δ) were cultured in YE to mid-log phase (+N) and transferred into MM-N medium (-N). The DNA content of each sample was analyzed by FACS. (Lower panel) Mating efficiency of *snf22*Δ, *ada2*Δ-*snf22*Δ, and *ada2*Δ strains. Equal numbers of cells of *h*$^{+}$ and *h*$^{-}$ strain were mixed and spotted on SPA and cultured at 30°C for 3 days. The genetic cross was repeated three times.

Supplemental Materials and methods

Synchronous meiosis culture of fission yeast

S. pombe strains used in supplemental data are listed in supplemental Table 1. For the synchronous meiosis, *pat1-114* mutant strain was cultured in MM medium containing nitrogen at 25 °C and transferred in MM lacking nitrogen at the density of 0.6 x 10^7 cells/ml and cultured further for 20 hour to arrest the cell cycle at G1 phase. The equal volume of MM+NH_4Cl (0.1%) medium was warmed at 37 °C and added to G1 phase arrested cell culture, and then culture temperature was changed to 34 °C to induce meiosis.

Northern analysis

The probes to detect transcripts of *rec6*, *rec7*, *rec8* and *rec12* were prepared from PCR products using a random-priming kit (Amersham Corp., Piscataway, NJ). The nucleotide sequence of each primer is as described below.

rec6-F; AATGCGATGTCAAATGC, rec6-R; TCAGTCTGCAGCCGAA,
rec7-F; CCCATCTGACGTGCATT, rec7-R; GTTGTGACGCAGTAATAC
rec8-F; CCCAAAGCAGTTACGAC, rec8-R; CGAACATGTGAATCCTTG
rec12-F; CCAGATTTGATGACGAG, rec12-R; TACTGAGTGCTTTCCAC

Determination of the ade6-M26 transcriptional initiation site by 5'- rapid amplification of cDNA ends (5'- RACE) analysis

Diploid *ade6-M26* strain (D20) was cultured in MM medium lacking nitrogen for 3 hours to induce meiosis, and the cells were harvested from 10 ml of the culture. Total RNA was prepared and 5'- RACE was carried out using a SMART RACE cDNA amplification kit (Clontech, Palo Alto, CA). The 5'- region of *ade6-M26* transcript was amplified by PCR using the universal primer mix included in the kit and the gene-specific primer, TCAATGGTGTAGTGACCTGA. PCR products were gel-purified (QIAquick; QIAGEN, Germany) and cloned into pCR2.1TOPO (Invitrogen, Carlsbad, CA). The sequence was then analyzed using GTGTTAATATGCTCAATTTC primer.

FACS analysis

The cells from a 1 ml culture were washed twice by distilled H_20 (dH_2O) and fixed with 70% ethanol overnight. Fixed cells were washed twice by buffer A (0.2 M Tris-HCl [pH 6.8], 0.05 M EDTA) and suspended in buffer A. The suspension was sonicated well and endogenous RNA was digested with RNase A (0.2 mg/ml). Buffer A, containing propidium iodide (20 μg/ml), was added to the cell suspension and allowed to stain the genomic DNA. The stained samples were analyzed by flowcytometry.

Supplemental Table S1 *S.pombe* strains used in Supplemental Results

K31 *h+ ade6-M26 his5-303*

K175 *h+ ade6-M26 his5-303 ura4-D18*

K176 *h- ade6-M26 leu1-32 ura4-D18*

TY24 *h- ade6-M26 gcn5::ura4 pat1-114 rad50s ura4-D18*

TY9 *h+ ade6-M26 gcn5::ura4+ uar4-D18 his5-303*

PKH138 *h+ ade6-M26 pat1-114 rad50S ura4-D18*

PKH265 *h+ ade6-M26 ada2::kanMX his5-303*

PKH267 *h+ ade6-M26 snf22::ura4+ uar4-D18 his5-303*

PKH268 *h- ade6-M26 snf22::ura4+ uar4-D18 leu1-32*

PKH273 *h+ ade6-M26 snf22::ura4+ gcn5::ura4+ uar4-D18 his5-303*

PKH279 *h+ ade6-M26 hrp1::ura4+ uar4-D18 his5-303*

PKH285 *h+ ade6-M26 hrp3::ura4+ uar4-D18 his5-303*

PKH293 *h+ ade6-M26 ada2::ura4+ uar4-D18 leu1-32*

PKH294 *h- ade6-M26 ada2::ura4+ uar4-D18 his5-303*

PKH309 *h+ ade6-M26 hrp3::ura4 pat1-114 rad50s ura4-D18*

PKH310 *h+ ade6-M26 ada2::ura4 pat1-114 rad50s ura4-D18*

PKH311 *h+ ade6-469 snf22::ura4+ ada2::ura4+ uar4-D18 his5-303 leu1-32*

PKH312 *h- ade6-469 snf22::ura4+ ada2::ura4+ uar4-D18 his5-303 leu1-32*

S13-I1 *h- ade6-M26 snf22::ura4 pat1-114 rad50s ura4-D18 leu1-32*

D45 *h+/h- M26/M26 rad50s/rad50s ura4D18/ura4D18 his5-303/+ +/leu1-32*

D64 *h+/h- M26/M26 rad50s/rad50ssnf22::ura4/snf22::ura4 ura4D18/ura4D18 his5-303/+ +/leu1-32*

D13 A1B5 *h+/h- M26/M26 snf22::ura4/snf22::ura4 ura4D18/ura4D18 his5-303/+ +/leu1-32*

Supplemental references

Cervantes, M.D., Farah, J.A., and Smith, G.R. (2000). Meiotic DNA breaks associated with recombination in *S. pombe*. Mol Cell *5*, 883-888.

Iino, Y., and Yamamoto, M. (1985). Negative control for the initiation of meiosis in *Schizosaccharomyces pombe*. Proc Natl Acad Sci U S A *82*, 2447-2451.

McLeod, M., and Beach, D. (1986). Homology between the *ran1+* gene of fission yeast and protein kinases. Embo J *5*, 3665-3671.
Young, J.A., Schreckhise, R.W., Steiner, W.W., and Smith, G.R. (2002). Meiotic recombination remote from prominent DNA break sites in *S. pombe*. Mol Cell *9*, 253-263.

Hirota et al. Supplemental Figure S1

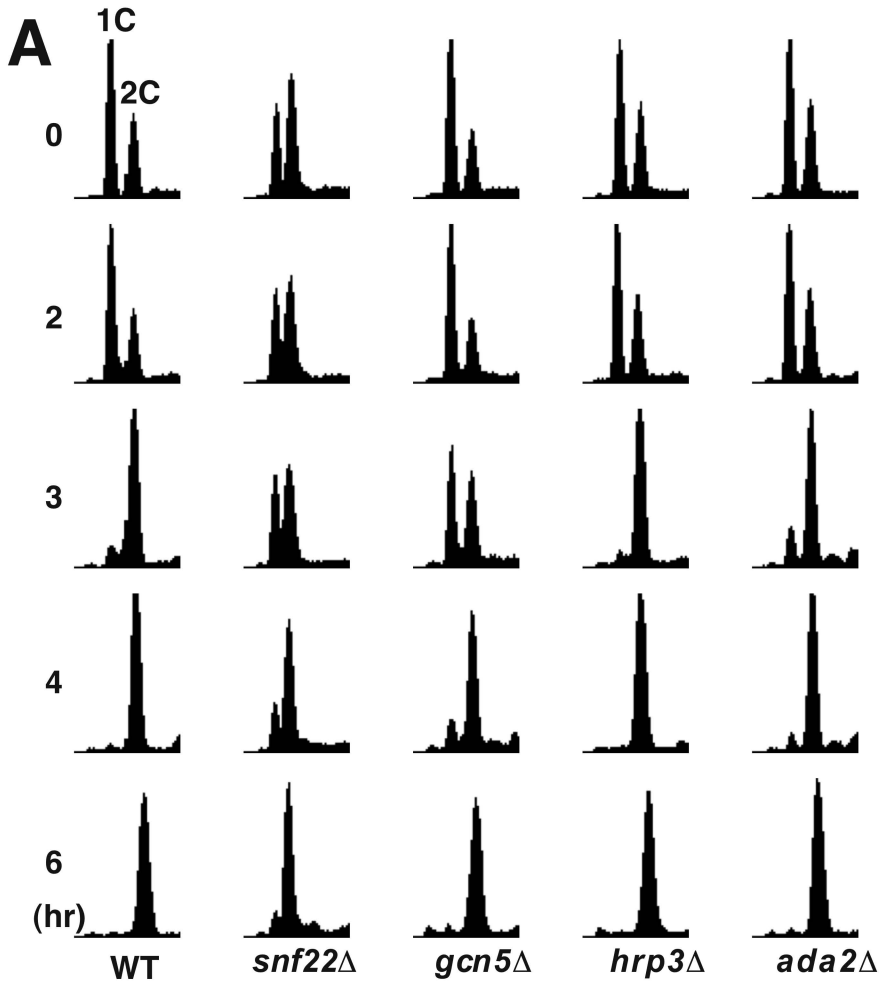

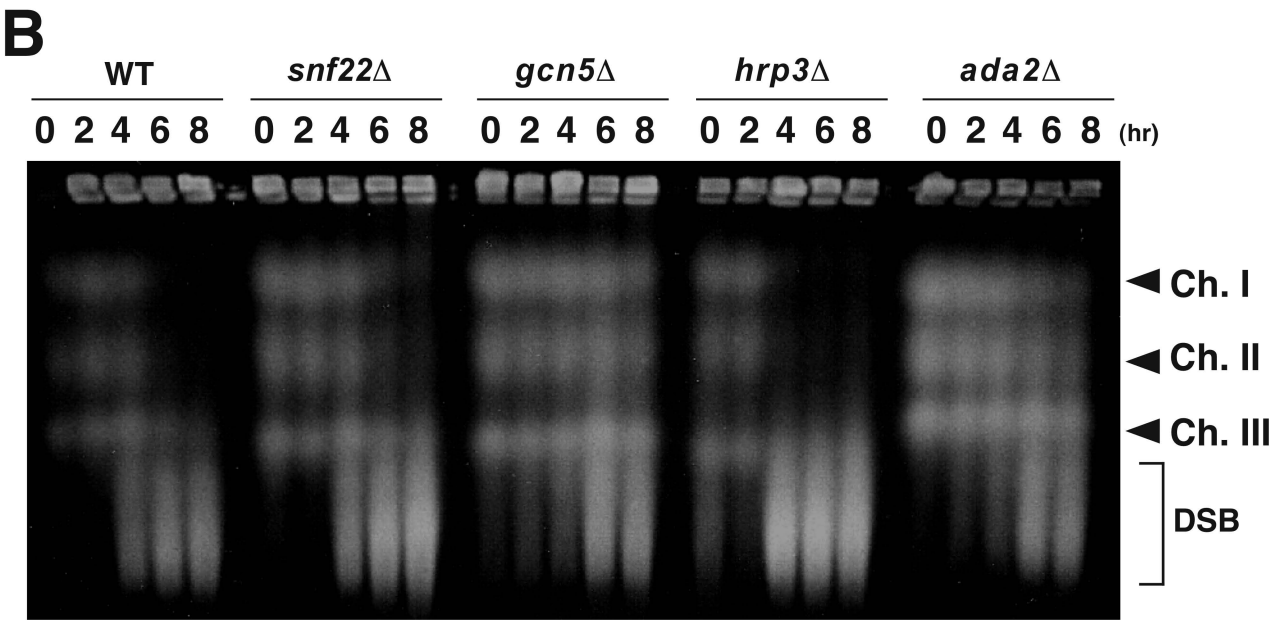

Hirota et al. Supplemental Figure S1

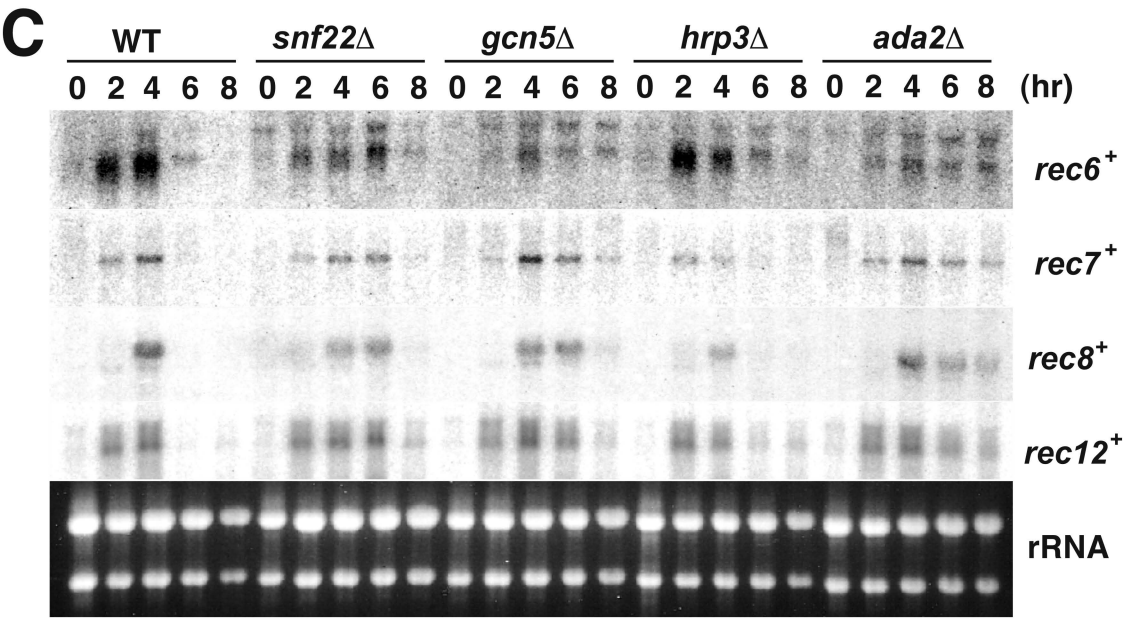

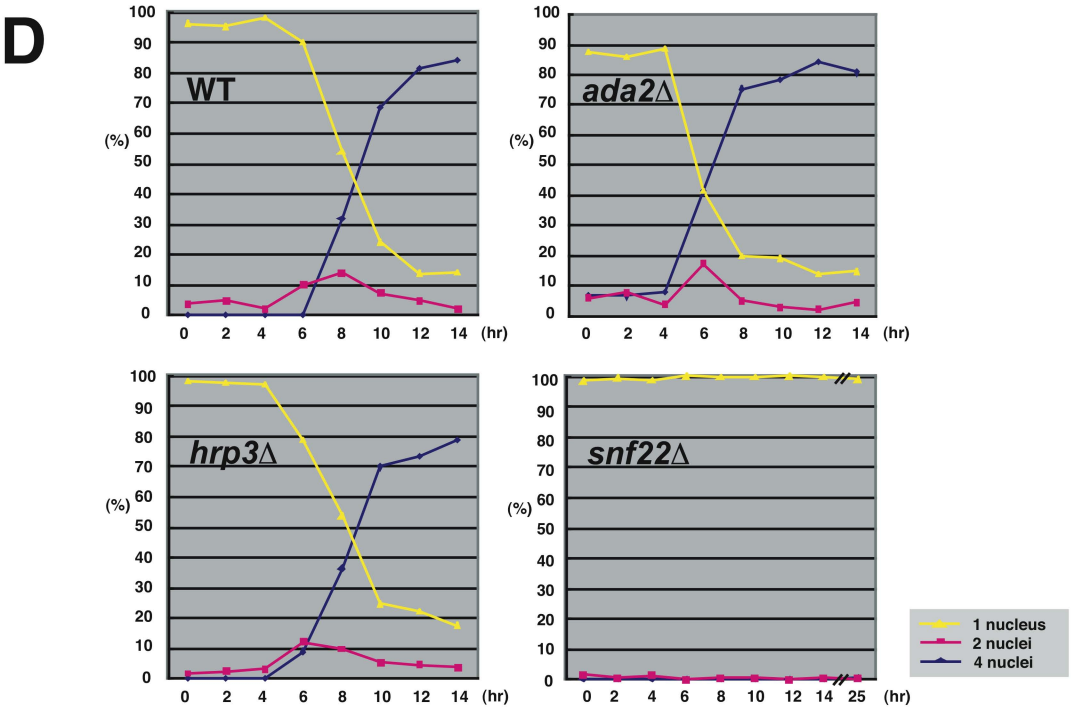

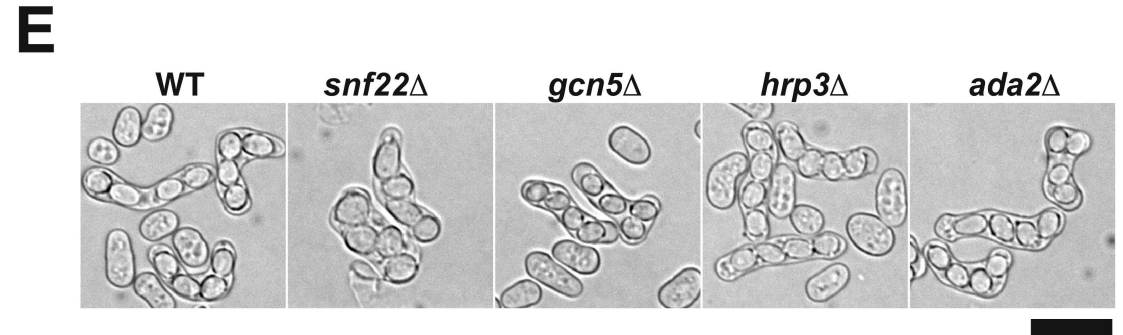

Hirota et al. Supplemental Figure S1

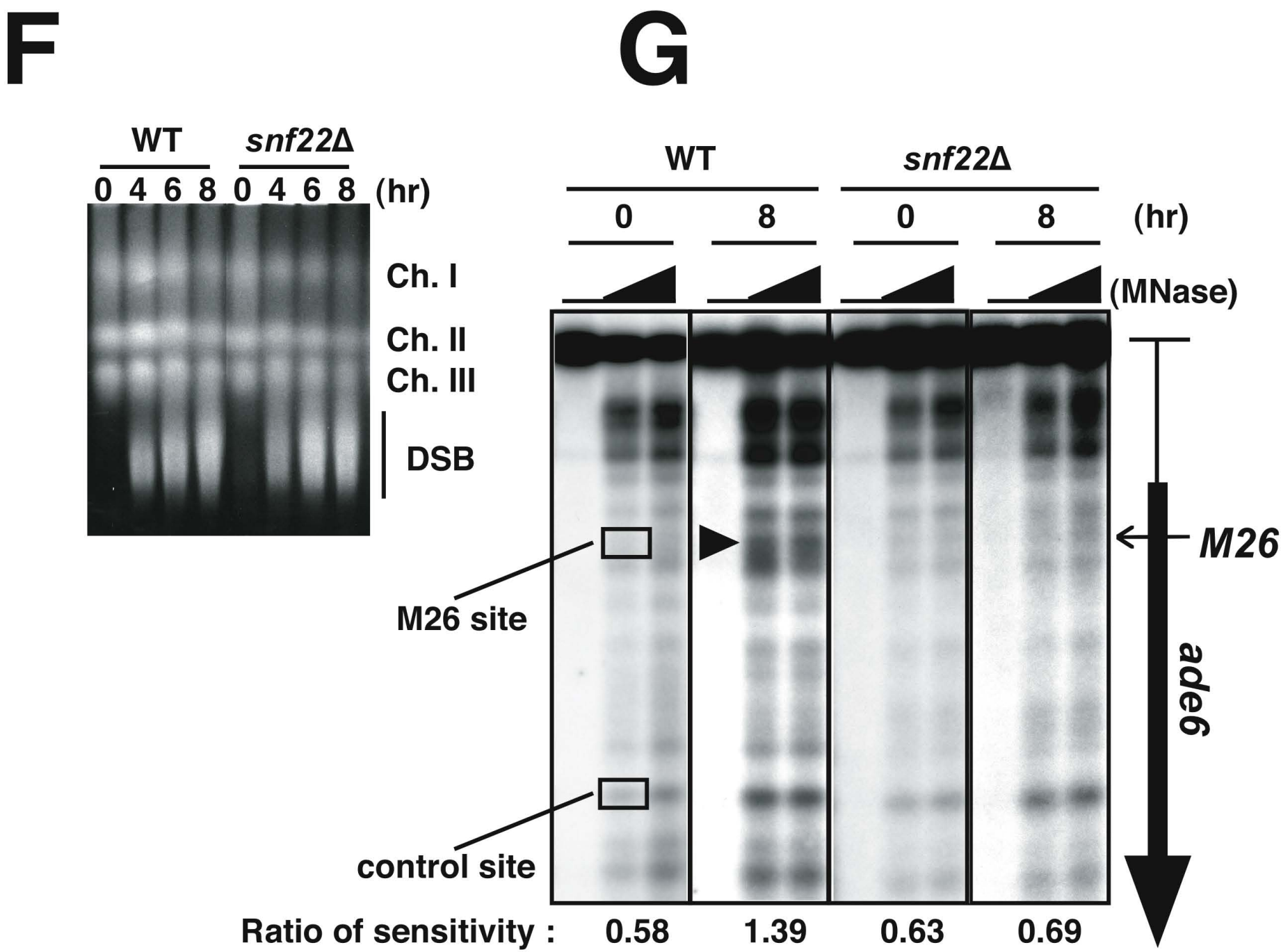

Hirota et al. Supplemental Figure S2

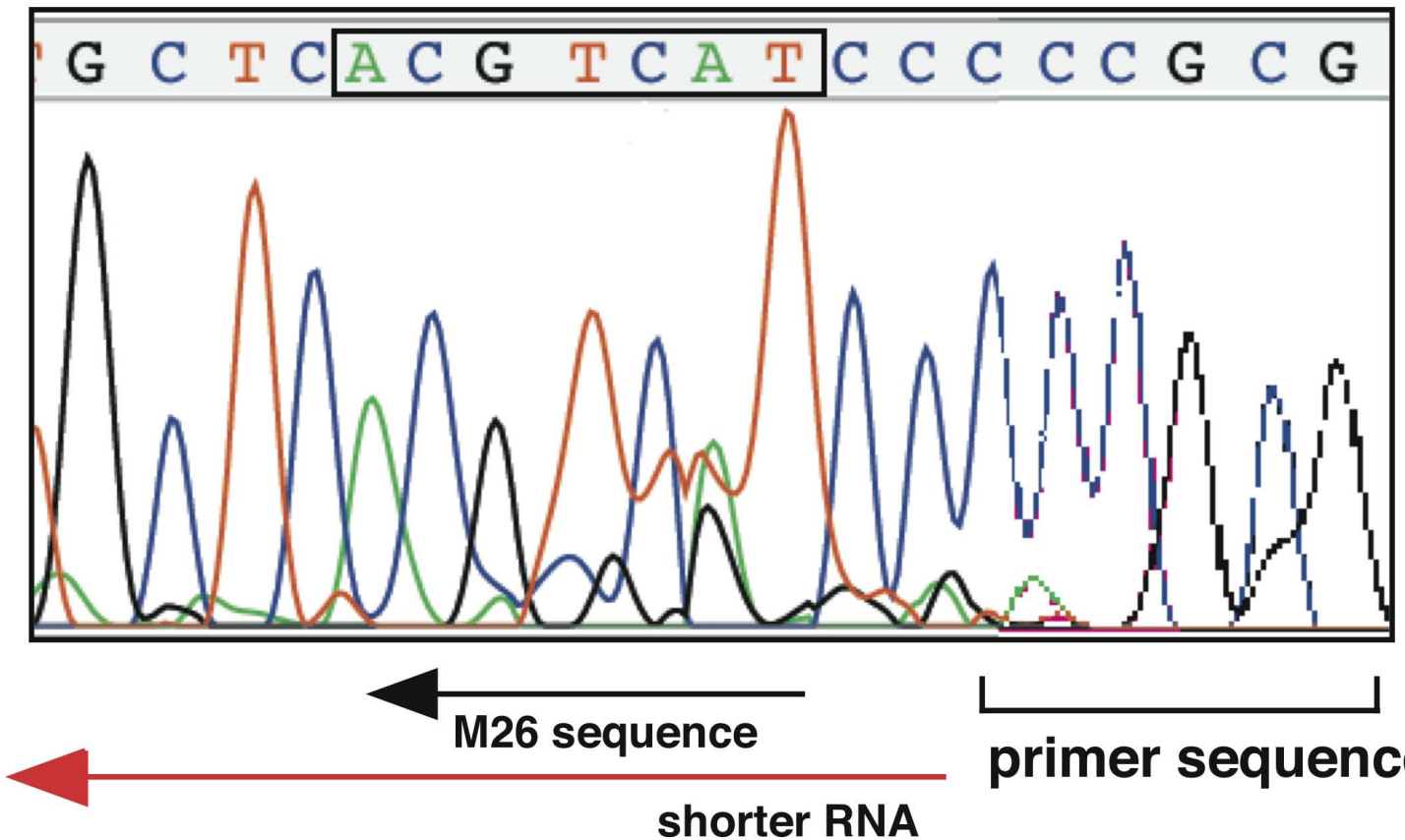

Hirota et al supplemental figure S3

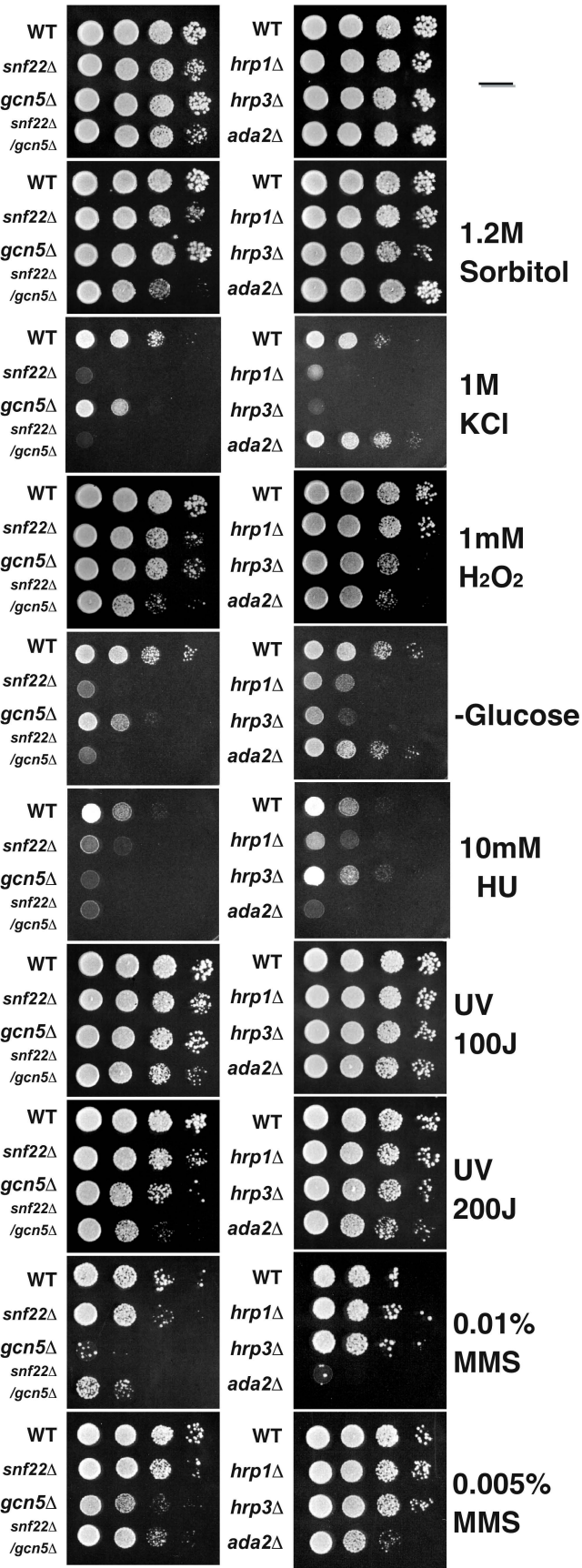

Hirota et al Supplemental figure S4